Thermochimica Acta, 139 (1989) 245–256
Elsevier Science Publishers B.V., Amsterdam – Printed in The Netherlands

HEAT CAPACITY MEASUREMENTS UNDER CONTINUOUS HEATING AND COOLING USING VACUUM ADIABATIC CALORIMETRY *

V.G. BESSERGENEV, Yu.A. KOVALEVSKAYA, I.E. PAUKOV and Yu. A. SHKREDOV

Institute of Inorganic Chemistry, Siberian Branch of the U.S.S.R. Academy of Sciences, Novosibirsk (U.S.S.R.)

(Received 11 July 1988)

ABSTRACT

An automated apparatus for measuring heat capacity by the method of vacuum adiabatic calorimetry is described. A procedure is also described for measuring heat capacity under continuous heating and cooling, which has been made possible with this apparatus. The possibilities of the apparatus are illustrated by a study of first- and second-order phase transitions in the rare earth metals terbium and dysprosium.

One of the key problems in the study of the thermodynamics of phase transitions is associated with establishing the form of the functional dependence of the thermodynamic quantities in the vicinity of the transition point. This problem places rather rigid requirements on the quality of the experimental data, i.e. their accuracy and details. In some instances, in the studies of both first- and second-order phase transitions, the required information can be obtained by the conventional adiabatic method with interrupted heating which appears to produce the most accurate data. Nevertheless, this method has at least three shortcomings: a loss in accuracy with reduction in the size of the temperature increment, which creates difficulties when working in the vicinity of temperatures where the function undergoes an abrupt change; a smoothing of the functional dependence over a finite temperature increment; and the impossibility of making measurements under conditions of decreasing temperature.

* Dedicated to Professor Edgar F. Westrum, Jr., on the occasion of his 70th birthday and in honour of his contribution to calorimetry and thermal analysis.

0040-6031/89/$03.50

However, a possibility for modification can be found in the method itself. Indeed, the formula for determining the heat capacity is

$$C = \frac{Q}{\Delta T} = \frac{N\Delta t}{\Delta T} \tag{1}$$

where Q is the energy input upon heating the calorimeter, ΔT is the temperature increment with the heat exchange taken into account, Δt is time of heating and N is the power. It is clear from the above formula that the value of the heat capacity can be obtained by measuring the power N and the time derivative of the temperature. Heat exchange is taken into account by the formula

$$C = \frac{N}{(\mathrm{d}T/\mathrm{d}t) - (\mathrm{d}T/\mathrm{d}t)_0} \tag{2}$$

where $\mathrm{d}T/\mathrm{d}t$ is the rate of heating and $(\mathrm{d}T/\mathrm{d}t)_0$ is the correction for heat exchange, i.e. for the temperature drift in the absence of a current through the calorimeter heater. Such a procedure allows the measurements of heat capacity to be carried out adiabatically under continuous heating. Corrections for heat exchange are obtained at the beginning and at the end of a thermogram and then interpolated to the moment of measurement. Usually, a temperature increment of 20–30 K involves only a small variation in the heat exchange correction value (within $\pm 10^{-3}$ K min^{-1}) and the linear interpolation is satisfactory. The rate of heating used to obtain a thermogram is usually about 1×10^{-2} K min^{-1}, and accounting for heat exchange with an accuracy to about 1%, will result in an error in the heat capacity value of $\lesssim 0.1\%$, which represents the maximum variation in $(\mathrm{d}T/\mathrm{d}t)_0$. Therefore, the accuracy of the heat capacity measurements is usually better than this and is not determined by the accuracy of the heat exchange correction value. Non-linearity of the variation of $(\mathrm{d}T/\mathrm{d}t)_0$ with temperature is mainly due to a non-linear change in the sensitivity of the thermocouple used to control the temperature of the adiabatic shield and to the temperature dependence of the calorimeter's thermal equivalent, both effects being, in the final analysis, determined by the quality of the system's design and construction.

It should be noted that the adiabatic conditions are necessary to minimize the uncontrollable heat flows. Actually, however, the conditions are quasi-adiabatic ones and the correction for heat exchange $(\mathrm{d}T/\mathrm{d}t)_0$ allows for deviations from the ideal conditions. In this discussion, we will not consider the problem of correcting for heat exchange at the moments when the current through the calorimeter is switched on and off. In the following arguments, it is the correction for heat exchange under steady-state conditions that is important, i.e. when the thermal regime has already stabilized. Also of importance is the fact that when the heat flow from the adiabatic shield to the calorimeter, and vice versa, is known and accounted for, its

presence will not have a substantial effect on the accuracy of the measurements.

On the basis of the above, let us describe a heat capacity measurement under a decreasing temperature. The method is based on the same principles as the adiabatic heating. The negative power, or heat flow from the calorimeter, is achieved due to a large shift of the adiabatic shield temperature relative to that of the calorimeter. The calorimeter cooling rate is set close to that of heating, about 1×10^{-2} K min^{-1}. In this case the heat capacity is determined from the formula

$$C = -\frac{N(T)}{dT/dt} \tag{3}$$

The power removed from the calorimeter can be measured by making the current through the calorimeter balance the negative temperature drift and is determined when the temperature drift in the system is zero. It should be noted that for this interpolation to be correct, the power should be measured at least three times during one thermogram because the variation in the power with time may be non-linear. Usually, the temperature dependence of the change in power within different temperature intervals is determined when calibrating the calorimetric apparatus.

There are, however, some drawbacks in the method of continuous heating or cooling. One of them is that the continuous change of temperature may give rise to temperature gradients in samples with poor thermal conductivity and this will increase the errors of the heat capacity determinations. To avoid this smaller temperature change rates have to be used which, in turn, lead to a decrease in accuracy and substantially increase the duration of the experiment. The problem of temperature gradients caused by heating the calorimetric cell can be partially solved by a suitable choice of cell design.

Therefore, because the continuous and interrupted methods have the same experimental equipment, the former method is a useful supplementary tool, especially effective in heat capacity measurements in the vicinity of a phase transition.

Consider now a practical application of the continuous method. Figure 1 shows a block diagram of the measuring section of the calorimetric apparatus. It consists of a calorimetric cell and two temperature-regulated shields [1]. Preliminary temperature stabilization of the current leads is performed with a copper ring whose temperature is also regulated. The use of two temperature-controlled shields with the proportional-integral law of regulation allows a decrease in the temperature gradients along the adiabatic shield and the calorimeter, and a reduction in the uncontrollable heat exchange on switching the heating on and off [2]. As usual, the measuring circuit consists of three main parts: the unit maintaining the adiabatic conditions; the unit measuring the calorimetric cell temperature and the

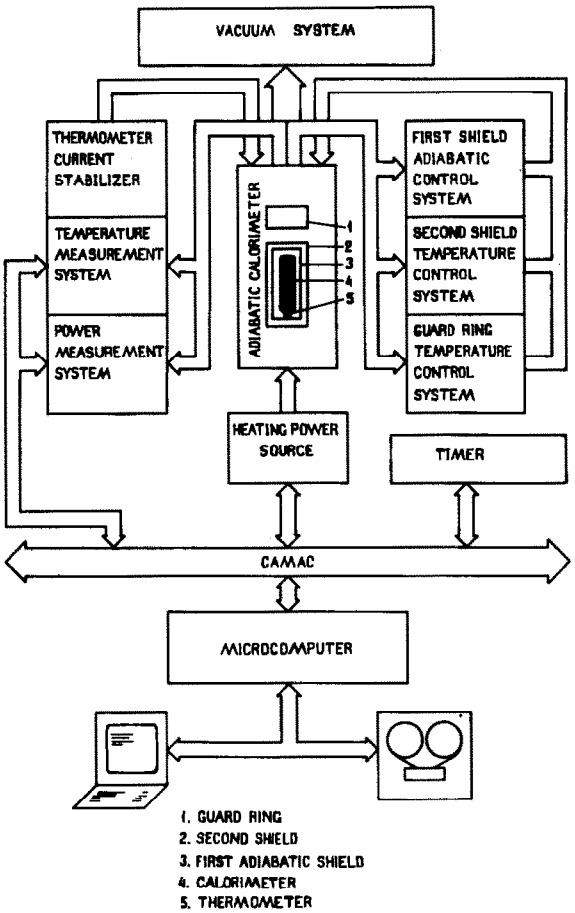

Fig. 1. Block diagram of the measuring section of the calorimetric apparatus.

power evolved at the calorimeter cell heater; and the electronics with a microcomputer controlling the heat capacity measurement process.

An important stage in a heat capacity measurement using interrupted heating is the analysis of the thermal conditions around the calorimetric cell for their steady-state. This is accomplished by periodical (usually once a minute) measurements of the temperature. The r.m.s. errors in the measured temperature values do not exceed 2×10^{-5} K, which is achieved by measuring the voltage on the platinum thermometer with a scatter of 30 nV and averaging over 50 measurements per minute.

The measurements and control of the outer devices are accomplished by means of a program which also links the computer with the external timer. According to the program, when a time signal arrives, a pre-set number of measurements is performed with the digital voltmeters in the platinum thermometer and cell-heater circuits, after which the values of time, power,

and temperature, i.e. t, N, T, are calculated. These three parameters are then transferred to the next programs for further processing.

Analysis of the temperature drift for linearity and, hence, for the steady state of the thermal conditions is usually performed by approximating 8–10 temperature points using ortho-normalized polynomials and statistical estimation of the significance of the coefficients of those polynomials with degrees greater than one [3]. If these coefficients are statistically insignificant, the thermal conditions are steady-state. In this case the calorimeter heater is switched on simultaneously with the signal from the external timer and heating takes place with a pre-set temperature increment. After switching off the heating, the temperature drift is checked for linearity and if the drift is linear the values of the average temperature and molar heat capacity are calculated. If the drift is not linear, the temperature is measured during the next minute and the analysis interval is shifted by one minute. This algorithm is repeated until the thermal conditions are steady-state. If the calorimetric experiment is not the first, the measured temperature drift is used as the final one of the preceeding calorimetric experiment and as the initial one for the forthcoming experiment. In the measurements of the temperature drift there may occur statistical outliers beyond 3σ where σ is the r.m.s. deviation of the measured values. In addition to such errors, the non-steady-state of the thermal conditions may sometimes result in a temperature drift with a "wave" which cannot be described by simple square or cubic functions. In this case, although the statistical analysis may indicate insignificance of the coefficients of a square or cubic polynomial, the temperature drift cannot be considered as linear. In order to exclude such a drift, the dispersion of the approximation is calculated simultaneously with the analysis of the coefficients of significance. The dispersion is then compared with an empirical value not exceeding twice the value of the dispersion in the case of a "good" temperature drift. Simultaneous application of these two criteria practically excludes the use of a "bad" drift and the subsequent decrease in accuracy during the automatic heat capacity measurements. Here again, the accuracy of the measurements is mainly determined by the quality of the calorimetric cells and shields as well as by the accuracy in maintaining the adiabatic conditions, and amounts to 1%, 0.15% and 0.06% for 12–20 K, 20–40 K and 40–312 K, respectively [1].

When heat capacity is measured by the continuous method the derivative dT/dt is calculated from the t, N and T data obtained as described above. To calculate the derivative, a pre-set number of points in the $T(t)$ curve is approximated by ortho-normalized polynomials, the degree of a polynomial being chosen using the Fischer criterion. The derivative is obtained by differentiating the approximation polynomial in the centre of the interval. Then the approximation interval is shifted by one point and the procedure is repeated. The heat capacity values are calculated by formula (2). Thus, the continuous method is largely based on the programs of the interrupted

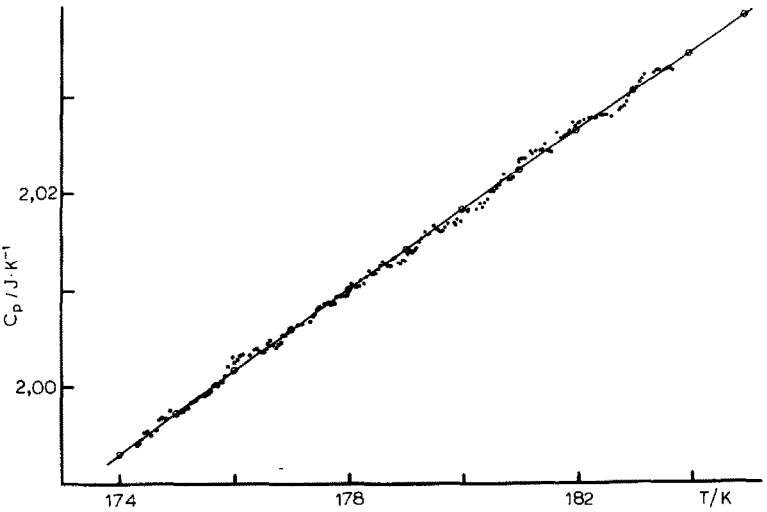

Fig. 2. Heat capacity of the empty calorimeter (●, continuous heating). The solid line was drawn through the smoothed values obtained by the interrupted method.

method. There is another source of error in the continuous method. At low temperature drift rates of about 10^{-3}–10^{-2} K min^{-1} the zero drift of the compensation amplifier becomes important. Uncontrolled zero drift of the amplifier maintaining the adiabatic conditions may affect the temperature drift and thus introduce a substantial error. For this reason, a nanovoltmeter with a guaranteed zero drift is used as the compensation amplifier.

Figure 2 shows the values of heat capacity measured by the continuous method. The solid line was drawn through the smoothed values of heat capacity obtained by the conventional interrupted method. The r.m.s. deviation of the heat capacity values from the smoothed curve is, in this case, 0.05%.

Let us now consider some applications of this method to the study of first- and second-order phase transitions. The anomalous behaviour of dysprosium's critical index (see eqn. (4), below) in the vicinity of the magnetic disorder temperature has been discussed earlier [4]. Possible reasons for this behaviour are: the effect of lattice compression; the presence of impurities in the sample; and the possibility of a first-order phase transition at the Néel point, T_N. It has been shown that none of these reasons was able to give a satisfactory explanation for all the available experimental data. It was possible to explain the observed features of the critical behaviour by assuming formation in the magnetic system of quasi-two-dimensional vortex structures, described by Kosterlitz and Thouless [5]. In a series of later studies [6–8], it was shown that the vortex structures also exist at $T < T_N$. The vortex state is metastable, and exists in a relatively small temperature interval approximately 5–10 K below T_N, when the sample is cooled down

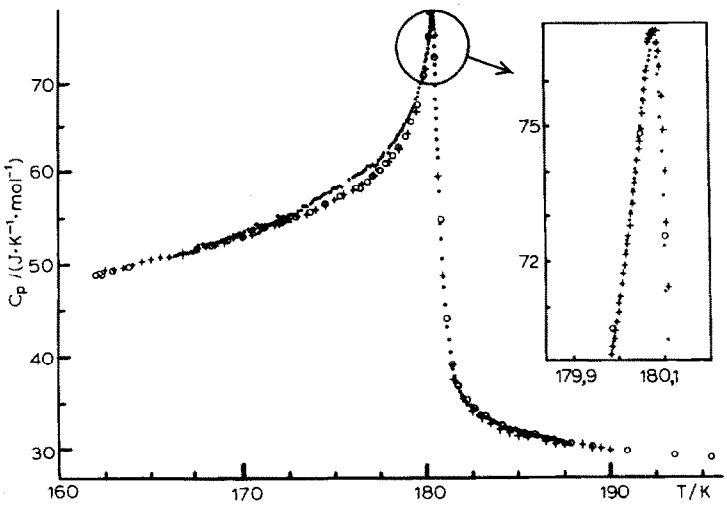

Fig. 3. Heat capacity of dysprosium in the vicinity of the magnetic disordering point: +, continuous heating; ●, continuous cooling; ○, interrupted method.

from the paramagnetic region. On further cooling, the vortex structure is destroyed and the magnetic structure of dysprosium becomes helical. If after this the sample is heated again, the helical structure is retained up to the magnetic-disordering temperature and signs of a vortex state appear only in the immediate vicinity of the Néel temperature. In the vicinity of T_N, hysteresis is observed in magnetic [6], lattice [7] and neutron diffraction [8] data. Recently, differences in electrical resistivity, i.e. in the electron scattering processes, have also been observed [9]. For each of these quantities the maximum of the anomaly observed on heating coincided with that observed on cooling, while the forms of the temperature dependences in the two runs were different.

In order to further investigate the thermodynamics of the vortex state we have undertaken a study of the heat capacity of a high purity dysprosium. The sample consisted of a set of small crystals which were obtained by double vacuum distillation. The ratio of the room to liquid helium temperature resistances, $R_{300}/R_{4.2}$, varied from 150 to 240. The amount of non-gaseous impurities was about 8×10^{-3} at.%. The total content of oxygen, nitrogen and carbon did not exceed 0.02 at.%.

The heat capacity was measured both by interrupted and continuous methods under heating and cooling conditions. The results are shown in Fig. 3. The density of the continuous data points shown in the main figure is reduced and all of the data are given in the inset. The average heating rate was about 0.015 K min^{-1}, and that of cooling was 0.012 K min^{-1}. It can be seen from the figure that the temperatures of the maxima of the anomalies upon heating and cooling coincide, which confirms the existence of a second-order phase transition in dysprosium. The values of heat capacity

obtained by different methods are also seen to coincide in the paramagnetic region at $T > T_N$ and at $T < 170$ K. In the temperature region $170 < T < T_N$, where the previous observations [6–9] indicated the occurrence of a vortex state upon cooling, the heat capacity values obtained upon heating and cooling are different. This difference in the heat capacity values is, in our opinion, due to the fact that the vortex state is energetically different from the helical state and is metastable in the given temperature region. It should, however, be noted that the difference is not large and appears to be determined by the long-wave region of the energy spectrum. This conclusion is based on the fact that the helical and magnetic vortex orderings have nearly the same short-range orders of the magnetic moments in planes. The difference becomes appreciable only at 5–10 interatomic distances, which corresponds to the long-wave region of the spectrum, and therefore manifests itself in the close vicinity of the disorder transition temperature where the correlation radius increases and where the theory predicts a predominant contribution from the long-wave fluctuations of the order parameter. Let us note here that the vortex state is only found in sufficiently pure samples [4]. Moreover, repeated cooling to temperatures below that of the ferromagnetic transition $T \simeq 90$ K, where the sample undergoes strong magnetostriction deformations, may result in the vortex state not appearing at all, even in sufficiently pure samples. This fact also indicates that a network of impurities or dislocations of a suitable average size may substantially distort the picture of a phase transition in the long-wave magnetic structure.

A similar phase transition study has been performed for terbium [10]. The sample was cut out from a block of single crystals with the main component content of 99.85% and the ratio of electrical resistances $R_{300}/R_{4.2}$ being 26. The C_p measurements were performed in a microcalorimeter having a volume of 0.3 cm^3 [11] using the continuous heating method. The sample weight was 1.19 g. The experimental data on C_p (about 600 points) were obtained in the temperature range from 227 to 267 K and the results are shown in Fig. 4. Random deviations of the C_p values obtained by the two methods of interrupted and continuous heating were, on average, about 0.3%. It can be seen that below the Néel point the heat capacity dependence is distorted by the nearby Curie point. Therefore, in the analysis of the critical behaviour the experimental data at $T > T_N$ and $T_N - T < 1.5$ K were used.

The magnetic component of the heat capacity $C_M(T)$ obtained from the experimental $C_p(T)$ data by extraction of the lattice heat capacity, was approximated by the power function

$$\frac{C_M}{T} = A + B\tau^{-\alpha} \tag{4}$$

where $\tau = |T - T_N|/T_N$, with testing of the adequacy and stability of the approximation towards variation of the number of experimental points. The

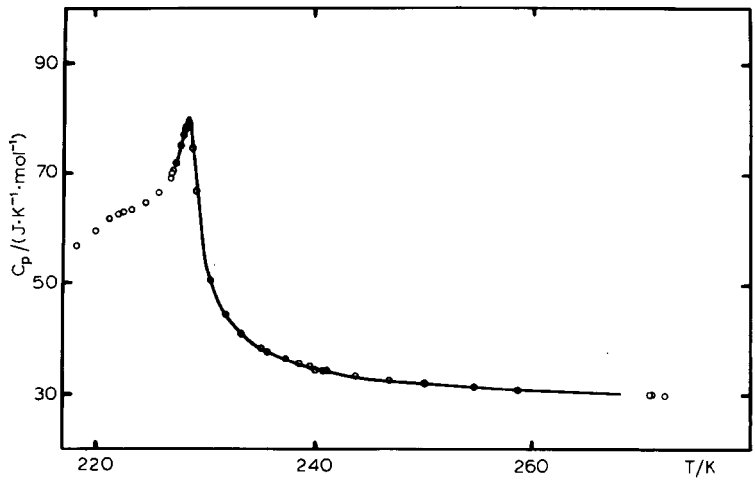

Fig. 4. Heat capacity of terbium in the vicinity of the magnetic disordering point: o, interrupted method. The solid curve was drawn through the points of the continuous heating data.

lattice heat capacity of terbium was represented by the heat capacity of non-magnetic lutetium which has lattice parameters close to those of dysprosium. The subtraction was performed in reduced T/θ co-ordinates where θ is the Debye temperature.

It was found that the description was adequate only at $2\text{K} < T - T_N < 15$ K. The values of α within this region were equal to 0.5 ± 0.3. For example, in the interval from 234.1 to 243.5 K, the value of α obtained from 100 points was equal to 0.5. Inclusion of higher temperature data immediately resulted in inadequacy of the approximation. Similarly, a shift of the left-hand boundary towards T_N, with the right-hand boundary being fixed, also results in inadequacy of description by eqn. (4) and a sharp increase in the critical index. The obtained values of α correspond, although with a large scatter, to those of the molecular field approximation. At $T - T_N < 2$ K, function (4) fails to describe the experimental data. By analogy with dysprosium [4], it can be expected that in the region of developed long-wave fluctuations, i.e. in the vicinity of T_N, the magnetic structure is quasi-two-dimensional and the thermodynamics is described within the Kosterlitz–Thouless theory

$$\frac{C_M}{T} = A + B\tau_1^{-2} \exp\left(-B/\sqrt{\tau_1}\right) \tag{5}$$

where $\tau_1 = |T - T_0|/T_0$, and T_0 is the Kosterlitz–Thouless temperature. It was found that approximation by function (5) is adequate in a small temperature range of about 35 experimental points. Displacement of this interval within the range from 228.3 to 231.1 K always gave an adequate description but the parameters in (5) changed. The size of the temperature

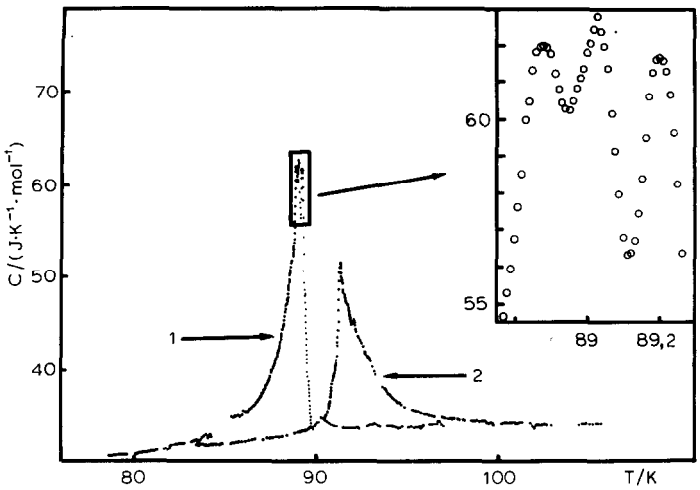

Fig. 5. Heat capacity of dysprosium in the vicinity of the Curie point. Continuous heating and cooling.

interval was 0.8–2.2 K depending on the density of points in the $C_M(T)$ curve. It was not possible to describe all data in the region 228.3–231 K by a single function of the type (5). Increasing the approximation interval or extending it beyond the given temperature region makes the description inadequate. Such behaviour of the heat capacity of terbium is qualitatively consistent with the results obtained on a sample of pure dysprosium [4] in the vicinity of the Néel point. This may be due to the fact that the helical magnetic structure period in terbium is greater than that in dysprosium and therefore the correlation radius increases to the required dimension (of the order of the magnetic structure period) only in the immediate vicinity of T_N. The long-wave properties also appear in the vicinity of T_N. However, for more substantiated conclusions, it is necessary that the heat capacity measurements be performed on more perfect samples.

Methods of measuring heat capacity using continuous heating and cooling have also been employed to study the first-order transition in dysprosium which occurs near 90 K. The results of these measurements are presented in Fig. 5. It can be seen that the $C_p(T)$ curves obtained on cooling (curve 1) and on heating (curve 2) differ substantially both in the extremum temperature and in their form. However, apart from these anomalies, the heat capacity values on heating and cooling coincide within the experimental error. It can also be seen that in the vicinity of the extremum, the $C_p(T)$ dependence in curve 1 splits into several anomalies. This is shown in more detail in the inset in Fig. 5. The anomalies may be due to the measurements having been performed on several samples.

The main problem in the study of the thermodynamics of a first-order phase transition is associated with the stability of the phases and the

mechanism of transition from one phase to another. The study of the first-order phase transition in dysprosium shows that its nature cannot be explained in terms of the formation of nuclei of the new phase with dimensions greater than the critical size and their further growth. In going from a helical to a ferromagnetic state, dysprosium undergoes substantial mechanical deformations due to strong magnetoelastic interaction. The mechanism of phase transition in such systems, involving formation of nuclei, has been considered in a number of theoretical works [12,13]. It was shown that at temperatures up to the lability point, i.e. the temperature of absolute instability, the formation of nuclei in such systems is energetically unfavourable due to complete dynamic striction blocking. Experimentally, the $C_p(T)$ curves show sharp peaks occurring in a very narrow temperature interval and resembling δ-functions. It is clear that the phase transition in dysprosium has a different nature. Indeed, even when dysprosium is in the helical state, there are domain boundaries between the sections of a helicoid having opposite directions of magnetic moment rotation [14] and in the sites where there is a disturbance in the phase of rotation. These regions have an uncompensated magnetic moment and may, apparently, function as nuclei of the ferromagnetic phase on approaching the phase transition temperature. Similarly, in the ferromagnetic state, the Bloch walls between the magnetic domains, where the magnetization vector changes its direction, can be considered as nuclei of the helical state and the first-order phase transition may be considered as an anomalous growth of such domain boundaries. In this case it can be expected that the region of the phase coexistence will be finite. Indeed, in a recent study on X-ray diffraction [15], such regions have been found following heating of a sample in the vicinity of the Curie temperature. As can be seen from Fig. 5, in our case regions of coexistence of the ferromagnetic and helical structures occur both upon heating and cooling; this is apparent in an asymmetry of the temperature dependence of the heat capacity. We believe, therefore, that this may be considered as favouring the proposed mechanism of the first-order transition.

The examples of the application of the continuous method for measuring heat capacity presented here illustrate its usefulness for a wide range of experiments. As pointed out above, the method can be especially convenient for studying phase transitions.

REFERENCES

1 I.E. Paukov, V.F. Anishin and M.P. Anisimov, Zh. Fiz. Khim., 3 (1972) 778.
2 Ya.V. Vasil'ev and A.F. Neyermolov, Zh. Fiz. Khim., 4 (1972) 1012.
3 D.J. Hudson, Statistics for Physicists, Mir, Moscow, 1970, p. 161.
4 E.B. Amitin, V.G. Bessergenev and Yu.A. Kovalevskaya, Sov. Phys. JETP, 57 (1983) 117.
5 J.M. Kosterlitz and D.J. Thouless, J. Phys. Chem., 6 (1974) 1181.
6 V.G. Bessergenev, Sov. Phys. Solid State, 26 (1984) 636.

7 E.B. Amitin, V.G. Bessergenev and Yu.A. Kovalevskaya, J. Phys. F, 14 (1984) 2935.
8 V.G. Bessergenev, V.V. Gogava, Yu.A. Kovalevskaya, A.G. Mandzhavidze, V.M. Fedorov and S.I. Shilo, JETP Lett., 42 (1985) 412.
9 J. Dudas, A. Feher and S. Janos, J. Less-Common Met. 134 (1987) L9.
10 E.B. Amitin, V.G. Bessergenev and Yu.A. Kovalevskaya, Fiz. Tverd. Tela (Kharkar/ Leningrad) 26 (1984) 1044.
11 K.S. Sukhovei, V.F. Anishin and I.E. Paukov, Zh. Fiz. Khim., 48 (1974) 1589.
12 V.G. Bar'yakhtar, I.M. Vitebskii and D.A. Yablonskii, Fiz. Tverd. Tela (Kharbar/ Leningrad), 19 (1977) 347.
13 V.G. Bar'akhtar, I.M. Vitebskii and D.A. Yablonskii, Fiz. Tverd. Tela (Kharkar/ Leningrad), 23 (1981) 1448.
14 S.B. Palmer, J. Phys. F, 5 (1975) 2370.
15 V.V. Vorob'ev, M.Ya. Krupotkin and V.A. Finkel, Zh. Eksp. Teor. Fiz., 88 (1985) 1780.